Mapping of short-range adhesive forces by scanning tunneling microscopy

U. Dürig and O. Züger

IBM Research Division, Zurich Research Laboratory, CH-8093 Rüschlikon, Switzerland

Detection of short-range interactions in combination with tunneling microscopy provides a means for characterizing the chemical nature of surfaces. Results are presented that demonstrate that carbon adsorbed on a rough, polycrystalline Ir surface can be detected on an atomic level.

Scanning force microscopy is by now a well-established surface imaging technique, in particular of nonconducting specimens.[1] So far, high resolution imaging has always been performed in the so-called contact operating mode, which means that the apex of the tip is actually pressing against the sample. In a typical force microscope, a soft lever to which a probe tip is attached serves as a spring for sensing the interaction between tip and sample. In order to achieve high sensitivity, levers are used with spring constants ranging from 0.1 to 10 N m^{-1}. As a consequence, force microscopy in the attractive force regime is difficult to perform, owing to the occurrence of a gap instability as the tip approaches the sample surface. In the attractive force regime the gradient of the tip-sample force is negative and increases in magnitude with decreasing distance. As soon as the magnitude exceeds the spring constant of the lever, the tip snaps towards the sample surface. At the new equilibrium the apex of the tip is actually in contact with the sample and exerts a substantial compressive force even though the net tip-sample force is still attractive. As a result of the repulsive forces at the apex, the gradient of the tip-sample force becomes positive which renders the tip-sample-lever system unconditionally stable. The latter property is a prerequisite for the proper functioning of the force microscope.

The amount of contact pressure exerted by the tip depends on the magnitude of the overall attractive interaction, which comprises short-range chemical interactions and long-range forces. The latter arise from static Coulomb interactions, i.e., owing to surface dipole layers and trapped charges, and from Van der Waals (VdW) forces. In some instances the VdW interaction can be eliminated almost completely by immersing the tip and sample in a liquid that matches their dielectric properties.[2,3] With this technique it is possible to operate the force microscope at extremely low loading forces of the order of pN provided that the tip and sample are mutually chemically inert, that is, if no short-range chemical forces come into play.

In this paper we focus on the interaction between metallic tips and metallic samples in ultrahigh vacuum (UHV). At a gap width of the order of 2 Å, the tip-sample interaction is dominated by short-range metallic adhesion forces that originate mainly from exchange-correlation effects in the region where the electronic wave functions of tip and sample overlap.[4] The interaction falls off exponentially with a characteristic length of ~ 0.5 Å, and the adhesive energy is of the order of 100–300 meV Å^{-2}. These parameters are also typical for other kinds of chemical interactions involving the overlap of electronic states.

Because of the exponential decay, short-range interactions probe essentially the very apex of the tip in a volume of atomic dimensions. Correspondingly, tip-sample forces and force gradients are of the order of 10^{-9} N and 10 N m^{-1}, respectively.[5] To avoid gap instabilities, stiff levers with a spring constant on the order of 100 N m^{-1} must be used for sensing tip-sample interactions in the short-range adhesion regime. However, deflections induced in such stiff levers are below 0.1 Å and thus are difficult to detect. On the other hand, interaction force gradients are easily measured by exploiting the dynamical properties of the lever. This method relies on the fact that the gradient of the force acting between tip and sample induces a shift of the resonance frequency of the lever. Interpretation of measured frequency shifts is straightforward as the dynamics of the first eigenmode of the lever are well represented by a simple spring model using a resonance frequency and spring constant that are identical to those of the lever.[6] The resonance frequency ω_r and interaction force gradient C_{TS} are then related as $\omega_r = \omega_0\sqrt{1 + C_{TS}/C}$, where ω_0 and C are the resonance frequency and spring constant of the free lever, respectively.

In contact force microscopy, the deflection of the lever provides a valid control parameter for feedback. Because of the stiffness of the tip-sample contact—the tip-sample force gradient is positive and comparable to or larger than the spring constant of the lever—the tip follows the surface of the sample at an almost constant distance irrespective of the lever deflection, which in turn is then basically a measure of the tracking error of the vertical positioning device. The situation is more complex in short-range adhesive force microscopy. Here, the spring deflection does not translate unequivocally into a measure for the gap width owing to substantial fluctuations of the local interaction depending on the chemical state of the surfaces. Particularly sensitive is the force gradient, which can even change its sign, a fact that is exploited in the present experiments but, on the other hand, renders any feedback system in a conventional force microscope unstable unless one resorts to elaborate adaptive schemes. Since we are interested in the interaction between metallic bodies, we can use the tunneling current as a measure for the tip-sample distance, and thus avoid the aforementioned problems.

Experiments are conducted using a standard UHV tunneling microscope. Vibrations of the lever are sensed by means of the tunneling current. Thermal noise and external feedback provide the driving force for the lever vibrations. Without external feedback, the lever vibrates pseudoperiodically
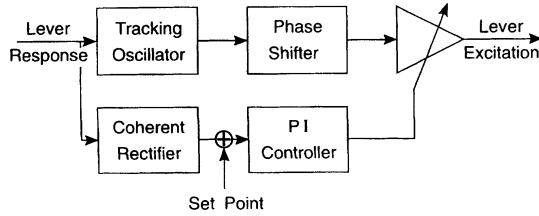
MAPPING OF SHORT-RANGE ADHESIVE FORCES BY ...

FIG. 1. Schematic diagram of the phase-controlled oscillator circuit.

with a mean amplitude $\Delta y^2 = k_B T/(C + C_{TS})$ as prescribed by the equipartition theorem. The frequency spectrum of the fluctuations is a Lorentzian centered at the resonance frequency ω_r and with a width ω_r divided by the Q factor of the resonance. The width of the frequency spectrum reflects the fact that the phase as well as the amplitude fluctuates in time. While amplitude fluctuations in principle have no effect on the frequency measurement, phase fluctuations limit its accuracy. The mean square frequency fluctuation due to random phase noise increases with the detection bandwidth W_B and is inversely proportional to the Q factor: $\Delta\omega_r = W_B \omega_r/2Q$.[6] The sensitivity of the frequency measurement is substantially increased if the lever is coherently excited by means of a linear feedback amplifier.[7] As a result of the feedback the apparent Q factor increases proportionally to the energy stored in the resonator scaled by the thermal energy. Thus, the accuracy of the frequency measurement improves with the vibration amplitude of the lever. Expressing the energy in the resonator in terms of its vibration amplitude and using a linear approximation for the resonance frequency yields

$$\Delta C_{TS}^2 \approx \frac{W_B k_B T C}{\omega_0 2Q \Delta y^2} \qquad (1)$$

for the mean square fluctuations of the force gradient measurement. In practice, nonharmonic terms of the interaction potential impose an upper limit of ≈ 0.5 Å on the vibration amplitude. This value is only eight times larger than the intrinsic thermal vibration for a force constant of 100 N m^{-1} of the lever. Typical Q factors of the levers are of the order of 200–400 in our experiments. Therefore the detection threshold for measuring interaction force gradients is of the order of 1 N m^{-1} times the square root of the normalized detection bandwidth W_B/ω_0. The levers employed in our experiments have a resonance frequency of the order of 1–2 kHz. Hence, force gradients can be measured with an accuracy of ≈ 0.25 N m^{-1} at a typical scanning tunneling microscopy (STM) data acquisition rate while scanning at one line per second.

For the feedback method to be useful it must be possible to adjust the gain so as to maintain a constant vibration amplitude. Furthermore, the oscillation frequency of the excited resonator must be identical to its resonance frequency. Unfortunately, the latter condition is in general not fulfilled, unless the driving force and the vibration of the resonator are exactly 90° out of phase.[6] Figure 1 shows the main components of the phase-controlled oscillator circuit. The scheme can be applied in any kind of force sensing environment that provides means to excite the sensor at its resonance fre-

quency and that allows the detection of the induced oscillations. Here, the lever is excited by means of a piezoactuator. A phase-locked loop (PLL) frequency detector is used to measure the frequency of the tunnel current modulation induced by the lever oscillation. The tracking oscillator of the PLL circuit also provides the driving signal for exciting the lever. A variable phase shifter allows the phase of the driving signal to be adjusted with respect to the lever response to compensate for propagation delays of the piezotransducer and the tunnel current measuring electronics. Thus, the proper phase relation can be established that yields an accurate tracking of the resonance frequency. The amplitude of the tracking oscillator signal is controlled by an amplifier whose gain is controlled by a separate feedback circuit. It consists of a rectifier for measuring the amplitude of the tunnel current modulation and a proportional-integral controller. An important feature of the circuit is the fact that the gain can assume positive as well as negative values depending on whether the vibration amplitude is smaller or larger than the set point, respectively. In the first case the relative phase between excitation and response of the lever is such that vibrational energy of the lever increases. In the second case, the phase is reversed, hence vibrational energy is dissipated. The latter property is extremely important as relaxation times would be prohibitively long without selective damping. In passing, we note that the phase-controlled oscillator method can also be used for distinguishing conservative from dissipative tip-sample interactions, a feature that is not yet exploited in experiments.

Probing short-range interactions by means of force gradient sensing in combination with tunneling microscopy provides valuable complementary information. The STM is operated in the standard constant current mode and the resonance frequency of the vibrating lever is measured simultaneously with the topography. Electron tunneling is determined by the overlap of the wave functions of electrons at the Fermi level E_F. Hence, to lowest order, the tunneling microscope probes the product of the state densities at E_F of tip and sample.[8] Interaction forces, on the other hand, involve all valence electrons; hence, they provide chemical information that is only marginally accessible by tunneling. A typical example for the latter is the contrast created by adsorbed atoms (or molecules) whose electronic states are shifted far away from E_F. Such atoms are almost invisible to the STM because the density of states at E_F is almost the same as that of the bare substrate. The situation is different for the interaction forces. Suppose that the atoms are covalently bound to the substrate, i.e., that all valence electrons are paired. Hence, the response of the bound atom to extra electrons will be similar to that of closed shell atoms, i.e., electrons will be expelled thus increasing their kinetic energy.[9] Therefore, one expects that such an adsorbed atom will give rise to a repulsive contribution to the total tip-sample interaction.

For estimating the order of magnitude of the effect, additivity of the tip and substrate electron densities is assumed. This premise is reasonable for sufficiently large tip-substrate distances, for which the tunnel resistance is greater than, say, 10 MΩ. This means that if the tip is above the adsorbed atom, the latter is embedded in an electron cloud which also comprises those electrons from the tip that have leaked out at

the tip adatom distance. The energy required for embedding a closed-shell atom in a free electron gas is of the order of $\varepsilon_0 \simeq 150$ eV per unit electron density (in atomic units).[10] The typical electron density within metals is of the order of $\rho_e \simeq 0.01-0.03$. The density decays exponentially into vacuum with a characteristic length of $\kappa^{-1} \simeq 0.5$ Å. Hence, for the atom-induced repulsive tip-sample force, one obtains values of the order of $\kappa\varepsilon_0\rho_e \ e^{-\kappa s} = (5-15$ nN$) \ e^{-\kappa s}$ and, correspondingly, for the force gradient $\kappa^2\varepsilon_0\rho_e e^{-\kappa s} = (100-300$ N m$^{-1})e^{-\kappa s}$. These values are comparable to their counterparts for the short-range metallic adhesive interaction, but with opposite sign. Therefore, the adsorbed atoms should produce an easily detectable repulsive signal in the force gradient image. Note, however, that in many instances the nature of the binding is more complex, and also includes delocalized electrons and charge transfer. Under such conditions, the adatom-induced tip-sample interaction will also comprise attractive dipole interactions as well as more complex embedding energies that need to be calculated by some first principles methods (see, e.g., Ref. 10).

To demonstrate the principle of force gradient mapping, we used a polycrystalline Ir lever as sample. Experiments were conducted under UHV conditions ($p \leq 3 \times 10^{-10}$ mbar). Tips were made from Ir wire, which was mechanically sharpened at one end. Final tip forming was performed *in situ*. For this purpose, a positive bias is applied to the tip using a constant current source. The current is set to 10 μA and the maximum tip voltage is limited to 800 V. The tip is first brought into contact with an Ir test sample. Then the tip is retracted such that a constant gap voltage of ≈ 700 V is obtained. The process is stopped when a steady state is reached. Quite frequently, this treatment will result in poor resolution as determined from tunneling images. The resolution is recovered, however, by applying a short (≈ 300 ms) positive voltage pulse (≈ 100 V) to the tip while tunneling. Tip forming is crucial for obtaining reproducible force gradient measurements, as they are extremely sensitive to contamination.

Ir levers a few millimeters long and half a millimeter wide were fabricated from thin (50 μm) sheet metal. They were extensively sputter-cleaned prior to experiments. Nevertheless, Auger analysis revealed that a residual contamination of carbon (notably the only one detected) equivalent to a few percent of a monolayer persisted. In addition, carbon coverage increased gradually at a rate of 0.2 ML per 24 h when the sample was left in the UHV chamber.

In the experiment, the tunnel resistance was adjusted to 10 MΩ ($V_T = 20$ mV and $I_T = 2$ nA), a borderline value for detecting short-range adhesion forces,[5] but which, on the other hand, provides a tunnel gap large enough to keep tip-induced modifications of the surface from being too severe (see below). The topography of a 100×100 Å^2 area of the sputter-cleaned Ir surface is shown in Figs. 2(a) and (b) as top view and gradient image, respectively. The corresponding force gradient map is shown in Fig. 2(c) whereas Figs. 2(d) and (e) show the force gradient as recorded in subsequent scans of the same area. The gray scale is such that dark and light tones correspond to -8 N m^{-1} and 0 N m^{-1}, respectively. The most striking features in the force gradient maps are the dark and bright spots with lateral dimensions of the order of 5 Å. These spots will henceforth also be termed as attractive
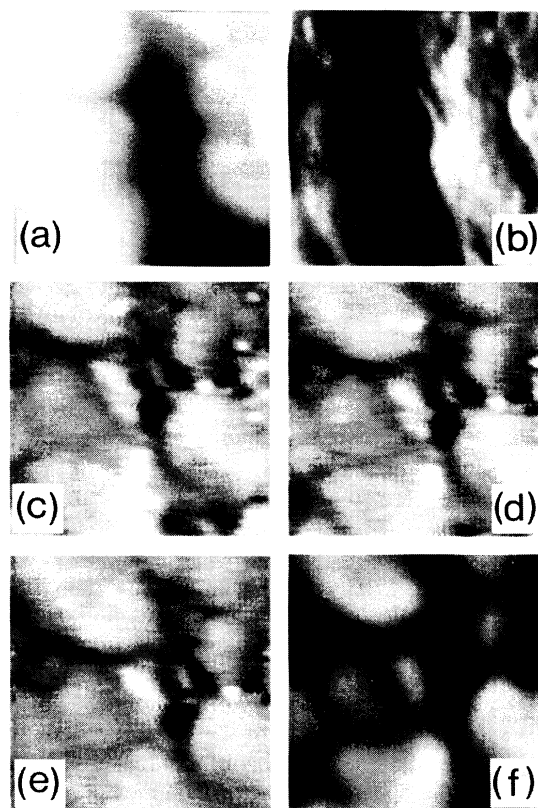

FIG. 2. 100×100 Å^2 area of a sputter-cleaned polycrystalline Ir surface. (a) Top view (dynamic range is 15 Å) and (b) gradient image of the topography. Force gradient map (dark, -8 N m^{-1}; bright, 0 N m^{-1}) recorded simultaneously with topography. (d), (e) Subsequently recorded force gradient maps of the same sample area. (f) Same as (d) but low-pass-filtered (dark, -6 N m^{-1}; bright, -2 N m^{-1}).

and repulsive sites in accordance with the change of the tip-sample interaction towards stronger and weaker interaction at the respective sites. Note that some of the bright spots visible in the force gradient map in Fig. 2(c) are absent in the subsequently recorded maps (d) and (e). In fact, repetitive scanning had a "cleansing" effect. With the exception of the one spot that coincides with pronounced topographic grooves, all repulsive sites had disappeared by the end of the fifth scan.

The Auger analysis suggests the identification of the repulsive sites with adsorbed carbon atoms (or clusters thereof). A repulsive force contrast is expected in view of the fact that small carbon clusters adsorb on the Ir surface by means of a covalent carbidic bond. This bond cannot be a strong one, however, as carbidic carbon spontaneously transforms into a graphitic form at higher coverage.[11] This also explains the relative ease with which the adsorbates are removed by the scanning motion of the tip. Consistent with the Auger results, the density of the repulsive sites is substantially higher for samples that had been left in the chamber for an extended period. Furthermore, by a careful comparison of topographic images we found that a slight depression with a depth of 0.3 Å was left behind whenever a repulsive site had been removed. A positive topographic contrast of that order

of magnitude was previously observed for carbon atoms ad-sorbed on Al(111) surfaces.[12]

The origin of the dark spots is unclear. These attractive sites were substantially less abundant than the repulsive ones. Most likely, they also arise from adsorbed atomic or molecular species of unknown composition. In addition to the well-localized features, one recognizes a characteristic modulation of the force gradient in the corresponding maps. In particular, the adhesive tip-sample interaction is enhanced along trenches that separate neighboring hillocks on the sur-face [see Fig. 2(f)]. The obvious correlation of topography and force gradient suggests that the enhancement arises from a geometrical effect, i.e., the exposure of the tip apex to a larger area of the sample while following V-shaped grooves. Geometry effects of that kind are expected to stem primarily from long-range VdW interactions which are always present in addition to the short-range forces.

This example clearly demonstrates the power of combin-ing interaction force detection and standard tunneling mi-croscopy. The tunneling current is only marginally sensitive to adsorbed carbon atoms. In order for these adsorbates to be detectable by STM alone, the topography of the substrate surface would have to be known *a priori* with an accuracy matching the height contrast they produce. This is definitely difficult to achieve for rough surfaces with a broad distribu-tion of corrugation amplitudes. Even when comparing sub-sequently recorded topographic maps, it is extremely diffi-cult to discern the places where adsorbed carbon atoms had been removed. The interaction force, on the other hand, pro-vides a clearly detectable flag that renders identification easy.

In conclusion we have shown that force microscopy ex-ploiting short-range interactions of chemical nature is fea-sible. However, stiff force sensing elements must be em-ployed which renders direct detection of tip-sample forces difficult. The problem is solved by resorting to a dynamic mode of operation that is sensitive to the interaction force gradient. By combining tunneling microscopy and force gra-dient sensing, identification of carbon atoms adsorbed on a rough, polycrystalline Ir surface has been achieved by virtue of characteristic changes of the short-range tip-sample inter-action induced by these adsorbates.

[1] For a review see, e.g., D. Rugar and P.K. Hansma, Phys. Today **43** (10), 23 (1990); D. Sarid, *Scanning Force Microscopy with Ap-plications to Electric, Magnetic, and Atomic Forces,* Oxford Se-ries in Optical Sciences, edited by M. Lapp and H. Stark (Ox-ford University Press, Oxford, 1991).

[2] N. Garcia and Vu Thien Binh, Phys. Rev. B **46**, 7946 (1992).

[3] F. Ohnsorge and G. Binnig, Science **260**, 1451 (1993).

[4] J. Ferrante and J.R. Smith, Phys. Rev. B **31**, 3427 (1985).

[5] U. Dürig, O. Züger, and D.W. Pohl, Phys. Rev. Lett. **65**, 349 (1990).

[6] U. Dürig, O. Züger, and A. Stalder, J. Appl. Phys. **72**, 1778 (1992).

[7] T.R. Albrecht, P. Grütter, D. Horne, and D. Rugar, J. Appl. Phys. **69**, 668 (1991).

[8] J. Tersoff and D.R. Hamann, Phys. Rev. Lett. **50**, 1998 (1983); A. Baratoff, Physica **172B**, 143 (1984); N.D. Lang, Phys. Rev. Lett. **56**, 1164 (1986).

[9] G.G. Kleinman and U. Landman, Phys. Rev. B **8**, 5484 (1973).

[10] S. Holloway and J.K. Nørskov, *The Binding of Adsorbates to Metal Surfaces,* Springer Series in Surface Science Vol. 2 (Springer, Berlin, 1984), p. 18.

[11] N.A. Kholin, E.V. Rut'kov, and A.Y. Tontegode, Surf. Sci. **139**, 155 (1984).

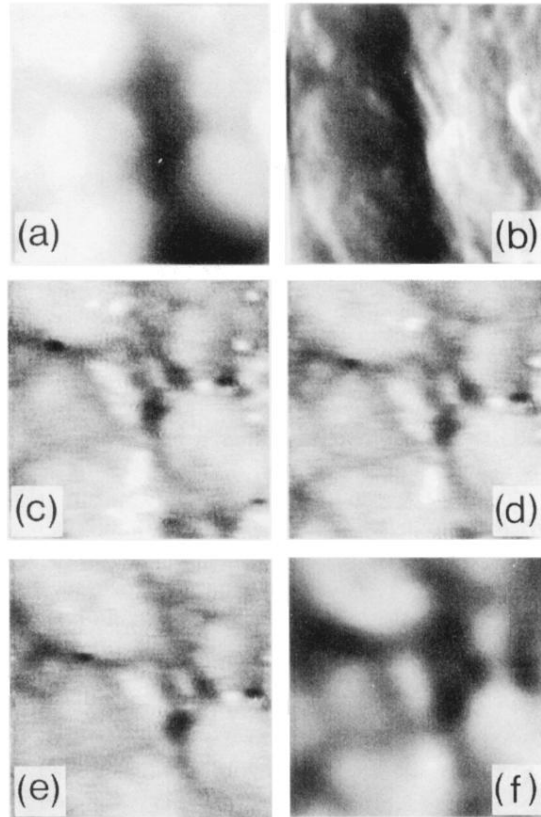[12] H. Brune, J. Wintterlin, G. Ertl, and R.J. Behm, Europhys. Lett. **13**, 123 (1990).

FIG. 2. 100×100 Å^2 area of a sputter-cleaned polycrystalline Ir surface. (a) Top view (dynamic range is 15 Å) and (b) gradient image of the topography. Force gradient map (dark, -8 N m^{-1}; bright, 0 N m^{-1}) recorded simultaneously with topography. (d), (e) Subsequently recorded force gradient maps of the same sample area. (f) Same as (d) but low-pass-filtered (dark, -6 N m^{-1}; bright, -2 N m^{-1}).